2015 IEEE International Conference on Robotics and Automation (ICRA)
Washington State Convention Center
Seattle, Washington, May 26-30, 2015

A Novel Volumetric Display using Fog Emitter Matrix*

Miu-Ling Lam, *Member, IEEE*, Bin Chen, *Member, IEEE*, and Yaozhung Huang, *Student Member, IEEE*

Abstract— **This paper presents a novel volumetric display based on projection on a non-planer and reconfigurable fog screen. Unlike conventional fog projection systems which produce 2D images on flat screens, our display scatters different parts of the projected image at different depth levels, thus allowing volumetric data to be displayed in the real 3D space. We constructed the fog screen with a 2D array of nozzles that are individually switchable, while the switching pattern is tightly synchronized with the video content. Our system is superior to many existing approaches at many levels. First, our display does not require head tracking, glasses or head-mounted devices while allowing high resolution, full color 3D image to be observed from wide viewing angles by many people at the same time. As compare with various existing approaches, our system is relatively easy to setup and low cost. Most importantly, our immaterial, mid-air display allows users to directly touch and manipulate virtual objects in 3D under marker-free and barrier-free settings which opens up immense tangible and creative interaction possibilities. In this paper, we provide the details of display mechanism and design prototype, as well as a constrained optimization problem to find the projection distance that can maximize the display resolution. A number of real display examples will demonstrate the performance of the proposed system.**

I. Introduction

3D displays have a wide range of applications in all disciplines, from art, design and entertainment, to engineering and scientific visualization, medical imaging and tele-presence. Many related technologies have been developed over the past decades and several works have made remarkable achievements. The autostereoscopic display developed in [1] used a rapid-spinning mirror to reflect the light field images from a high-speed projector and render a 360º observable image. Similar mechanism has been employed by [2], [3] and many other swept-volume displays to produce a series of fast-moving slices of the 3D object and base on human's persistence of vision POV to fuse the slices into a single 3D image. The display volume of these systems are usually small and enclosed in a container that is not reachable by users. [4, 5] used laser-plasma scanning to create an array of illumination points in mid-air. The display can only produce sparse (low resolution) and single-color luminous points. Also, the use of high power laser beam would induce safety concerns. Recently, Pixel Dust presented in [6, 7] used acoustic-potential field to trap and levitate small, light-weight objects by standing waves and create patterns for projection. This approach cannot be used for high-resolution volumetric display as only a low-density, 2D layer of particle pattern can be created at a time. inFORM [8] is a 2.5D shape display with 30x30 motorized pins that combines a Kinect-projector system for tangible interaction.

There are a number of interesting research works that used fog or other immaterial medium, such as water, smoke and particles, as projection screens to create unencumbered 3D visuals. [9] presented a walk-through fog display that could create depth cue by head tracking and rendering corrected perspectives. This system can only accommodate a single user and wearing infrared LED headset is required for the camera to detect the viewer's location. A technique called depth-fused 3D (DFD) [10] creates 3D perception by superimposing two images on two transparent screens at different depths while varying the luminance [10]. Therefore, DFD is suitable to be used with mid-air, immaterial displays such as fog screens. In [11], the same researchers from [9] used the generalized form of DFD and put two fog screens in multiple configurations to create 3D perception. However, this approach is, again, viewpoint-dependent and demands precise tracking of viewer's position. Also, it can only accommodate one viewer at a time. Besides, motion parallax is another technical for creating 3D perception. [12] presented a multi-viewpoint fog display that uses multiple projectors to project multiple images of the same virtual object from different viewpoints onto one cylindrical fog screen. When walking around the display, observers can perceive the 3D shape of the object based on motion parallax. The angle of projection between each projector for this approach should be kept small enough to avoid "gaps", thus many projectors are needed to facilitate a wide observable angle. [13] proposed a multi-layered water drop display that uses a projector-camera system to synchronize the valves and image. This system requires high-speed camera and compute-intensive control with GPUs to achieve precise drop synchronization. Besides, the drawback of using water drop is that, it is difficult to achieve high resolution display as each water drop represents only one pixel. Moreover, handling water is less convenient and infrastructures including drains and waterproof measures are required. The droplet size of fog or mist makes it easily disperse and evaporate into the air, thus fog screen can be used in all venues with effortless handling.

The objective of this piece of work is to create a high-resolution, scalable and low cost volumetric display that can be viewed by multiple simultaneous users and facilitate barrier-free, reach-through interaction. In this paper, we first describe the basic mechanism of the proposed fog display

* Research supported in part by the Croucher Foundation under Grant 9500016 and City University of Hong Kong under Grant 6980117 and 6987028.

M.-L. Lam is with the School of Creative Media and the Centre for Robotics and Automation, City University of Hong Kong, Kowloon Tong, Kowloon, Hong Kong: phone: +852-3442-2844; fax: +852-3442-0408; e-mail: miu.lam@cityu.edu.hk).

B. Chen is with the School of Creative Media, City University of Hong Kong, Kowloon Tong, Kowloon, Hong Kong (e-mail: binorchen@gmail.com).

Y. Huang is with the Department of Mechanical and Biomedical Engineering, City University of Hong Kong, Kowloon Tong, Kowloon, Hong Kong (e-mail: xiaozhun512@gmail.com).

and the design details of our prototype system. We also provide a simple calibration method in order to obtain all the required parameters for projection mapping onto different depth levels of fog. The proposed method also simplifies the original 3D-to-2D transformation problem to 2D translation and scaling of pixel coordinates. We then formulate a critical projection distance to avoid fog occlusion, and the optimal projection distance using the display resolution as the objective function under realistic contraints. Finally, we evaluate this piece of work by displaying static objects and animations. We also verify with an illustrative example that making the projection distance greater than critical projection distance can successfully solve fog occlusion issue and elimate unwanted artifacts. This paper concludes by giving the briefs of a few directions for further developments of this project.

II. METHODOLOGIES

A. Preliminaries

This subsection describes the mechanism of the proposed volumetric display and provides the notations and assumptions used in this paper. As shown in Fig. 1, the system consists of a calibrated projector and a matrix of fog emitters that produces columns of upward-flowing laminar fog. Each fog emitter is individually switchable and controlled using a microcontroller (Arduino [14]). When a fog emitter is switched on, its laminar fog forms an immaterial screen that scatters the light being projected onto it. A clear and bright image can be observed from forward and reverse directions along the projection axis owing to Mie scattering. The switching pattern of fog emitters is tightly synchronized with the image content.

Suppose the fog emitter matrix consists of m column (in x direction) and n rows (in z direction). The projection image is vertically divided into m segments, while each segment i is associated with a designated depth (image plane j in Fig. 2) for projection. At any time instant, only one of the n fog emitters per column is activated, thus the corresponding image segment will be formed only at its designated depth. Activating fog emitters in different columns at different depths will create a non-planar fog screen that can be used for displaying volumetric data in real physical space. We have developed a software to automatically transform the image segments in order to correct the distortion arising from the projective geometry on the non-planar screen. When the system is used to display dynamic content such as 3D video, animation and interactive game, the software sends synchronized switching pattern to the microcontroller so that the fog screen elements are reconfigured accordingly.

We fix the origin of the world coordinate system at the centroid of the display volume. The projector is precisely aligned such that its coordinate system is in a pure z-translation from the origin of the world coordinate system (projector's principal axis overlaps the world z-axis). The distance between the projector and the fog screen is denoted by d. The width, length and height of the display volume are denoted by W, L and H respectively, where H is obtained by measuring the minimum height of fog that can produce clear image. We assume that the fog nozzles are evenly distributed. The nozzle spacing in x and z directions are denoted by δ_x and δ_z. Given the fact that only one fog emitter per column is activated at a time, we define a fog vector:

$$f = (f_1, f_2, \ldots, f_m)^{\mathrm{T}}, \quad \text{where } f_i = j \in [1, n]. \quad (1)$$

When displaying animation, f is input as a time varying vector used for the synchronization between the fog emitter matrix and the dynamic image content. The computer reads the sequence of fog vector and switches on only the fog emitters at column i and row j as specified by (1). Let $X=(x, y, z)^{\mathrm{T}} \in \mathbb{R}^3$ be a point in the world coordinate system, and $\boldsymbol{u}=(u, v)^{\mathrm{T}} \in \mathbb{R}^2$ denotes the pixel coordinates of the image of point X in the projection plane. Since x determines i (segment/column index) thus j (depth/row index) by (1), this turns out to constrain the z-coordinate of X. In other words, given a fog vector f, we can transform the original problem of 3D-to-2D mapping to pure 2D translation and scaling of each of the m image segments.

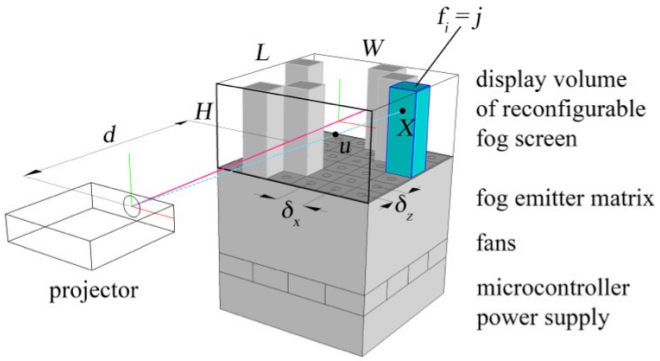

Figure 1. Volumetric display system with reconfigurable fog screen elements

B. Calibration

In order to map the projected image correctly to the non-planar fog screen, the projector's pose and parameters must be carefully calibrated. We propose a simple and effective method to align and calibrate the projector. The procedures are described below:

Step 1. Align principal axis with world z-axis

Two checkerboards were attached to the front and rear planes of the displayable volume. We projected a cross pattern (Fig. 2) on top of both checkerboards. The projector's position and orientation are adjusted such that the cross pattern and its center align precisely with both checkerboards. This procedure can effectively align the projector's principal axis with the world z-axis. It strictly constrains the projector's orientation and x-, y- locations while leaving only 1-DOF for it to translate along the z-direction. We will discuss a critical projection distance and the formulation of optimal projection distance in Section II.D. The projector's focal point is set to the origin of the world coordinate (centroid of display volume).

Step 2. Measure intrinsic parameters and distortion coefficients (optional)

We used a calibrated camera and the code given by [15] to calibrate the projector. The projector's intrinsic parameters as well as the radial and tangential distortion coefficients were obtained and applied for reprojection. However, we

found that the lens distortion and skew coefficient are insignificant in our case. Also, Step one has already aligned the principal and the focal points. This step is optional.

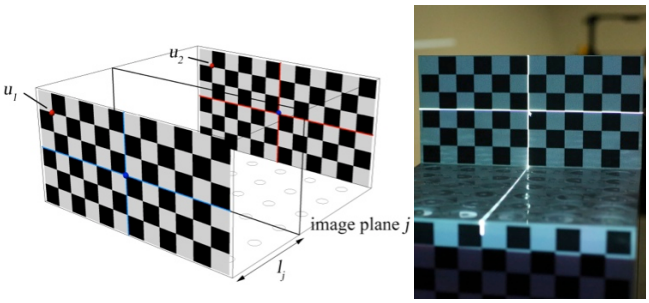

Figure 2. Cross and checkerboard patterns projected on front and rear planes of display volume for projector calibration.

Step 3. Compute projection distance and field of view

The final calibration step is to measure the actual projection distance d and the horizontal pixel dimension M_0 on the front plane. These parameters will allow us to evaluate the display resolution (total number of voxels) and map any point from world coordinate to pixel coordinate. M_0 can be easily measured by reading the pixel coordinates on the left and right edges. To accurately measure d without the use of expensive distance sensing equipment. We project a checkerboard pattern on the front plane and scale the pattern while fixing the center so that the projected checkerboard overlaps perfectly on the printed checkerboard. The pixel coordinate u_1 is saved. We then apply the same procedure on the rear plane and save the pixel coordinate u_2, where u_1 and u_2 are related by $u_1 = su_2$ and s (>1) is the scaling factor. The projector distance can be computed by:

$$d = \frac{L}{s\text{-}1} \tag{2}$$

Notice that, in (2), d is independent of W and H. Let θ_x and θ_y be the horizontal and vertical field of view (fov) of the projector, we have:

$$\theta_x = 2\tan^{-1}\left(\frac{MW}{2M_0 d}\right),\ \theta_y = 2\tan^{-1}\left(\frac{NW}{2M_0 d}\right) \tag{3}$$

where M and N are the native pixel dimensions of the projector. Note that, projectors usually have a claimed fov or throw-ratio provided by the manufacturers. (3) provides an evaluation and we can obtain an accurate measure with a large sample size. Furthermore, the scale s_j (<1) of each image plane j relative to the front plane can be expressed by

$$s_j = \frac{d}{d+l_j},\ \text{where}\ l_j = \frac{1}{2}[L+(2j\text{-}n\text{-}1)\delta_z] \tag{4}$$

l_j is the distance of image plane j from the front plane.

Thus, given the fog vector $f = \{f_i\}^{\mathrm{T}}$, image segment i should be resized by scale s_j where $f_i = j$. Then, the pixel coordinate of the center of image segment i is translated to the pixel coordinate u_{ij} of the nozzle of the i-th column and j-th row, which can be solved by simple trigonometry:

$$u_{ij} = \frac{(2i\text{-}m\text{-}1)\delta_x s_j M_0}{2W} \tag{5}$$

C. Design and Fabrication of Prototype

Fig. 3 shows the design of our fog display prototype. The fidelity of any fog display system highly relies on the steadiness of fog flow because turbulent flow (shown in Fig. 4(a)) will cause severe image distortion from off-axis viewing angles. To ensure laminar flow (Fig. 4(b)) while achieving closely-packed arrangement of fog emitter matrix, we used a triple-deck structure to position all the components as shown in Fig. 1. The microcontroller and power supply are placed in the bottom layer where there are also ventilation holes for air intake. An array of electric fans Fig. 3(b) are placed in the middle layer to bring accelerated airflow continuously from the base to the top layer.

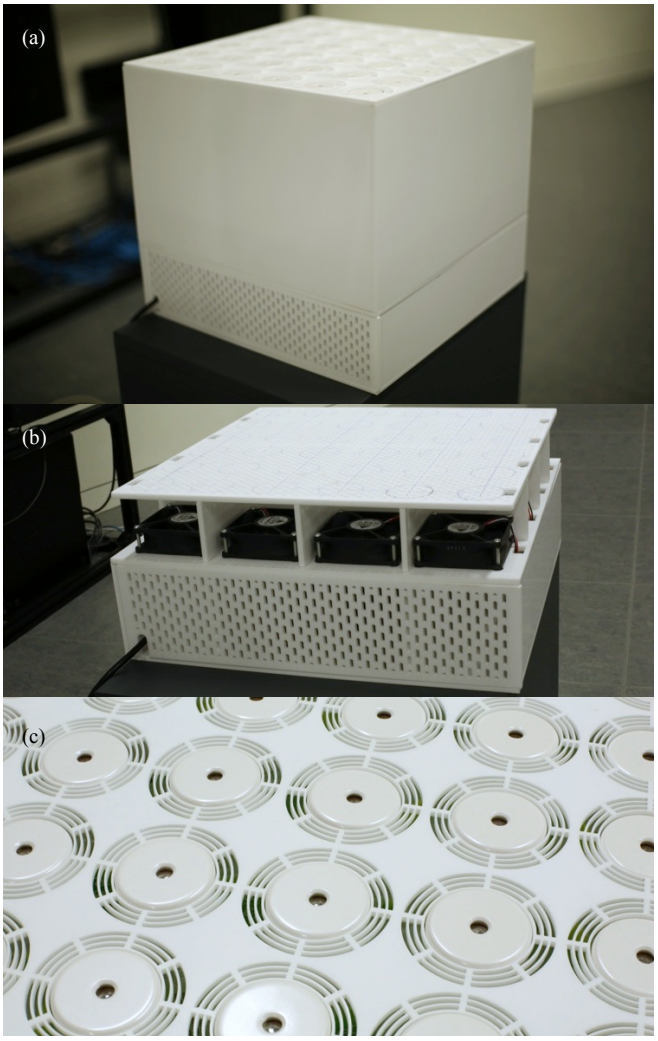

Figure 3. The prototype 3D fog display: (a) The container of triple-deck internal structure (b) fan array (c) details of nozzle array and arc-shaped vent holes.

The top layer (Fig. 3(c)) contains a matrix of humidifiers that use ultrasonic piezoelectric discs to generate high frequency oscillation in a film of water and produce microscale droplets that suspend in the air. Each humidifier is attached to a sealed water bottle with a cylindrical sponge to act as capillaries and supply water continuously to the piezo

disc. There are arc-shaped vent holes around each nozzle on the roof of the structure to ensure even airflow around each nozzle to limit the droplet spray angle. The packed, parallel pipe structure as used in many commercial fog display systems can also be added the air outlet to further enhance laminar flow. Directed airflow will also help the fog to reach higher. As shown in Fig. 4(a), when the fans are turned off, the mist produced is under turbulence without guided airflow. When the fans are on (Fig. 4(b)), fog stream becomes upright and can reach higher position.

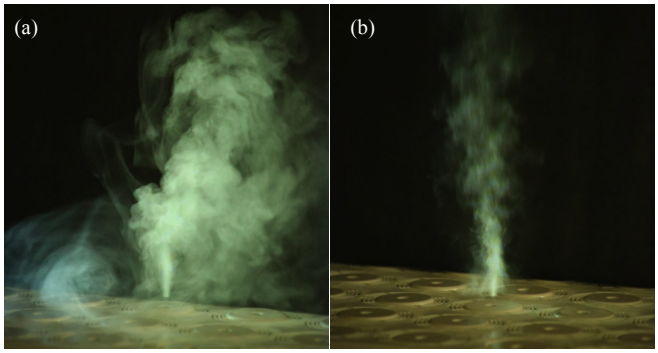

Figure 4. Comparison of fog produced with/without fans (a) turbulent flow without fans (b) laminar flow with fans.

D. Optimal Projection Distance

The resolution of volumetric display, that is the number of distinct voxels that can be displayed, provides an important quantitative measure for evaluation. As previously mentioned, the projector pose remains 1-DOF (projection distance d) along its principal axis. Placing the projector further away from the fog screen will waste a large projection area outside of the display volume and significantly reduce the display resolution. Thus, the projector should be placed as close to the fog screen as possible to maximize the number of usable pixels. However, there are also some constraints, such as to ensure the entire display volume is covered by the projection region. Also, if the projection distance is too short, the fog display may suffer from undesirable artifacts due to occlusion among the fog screen elements. To address this, we have formulated the minimum distance, called the critical distance $d_{critical}$, to avoid such occlusion. The details will be discussed in Section II.D.ii. Putting all these considerations into account, we can obtain an optimal projection distance d^* by solving the constrained optimization problem to be described in Section II.D.iii.

D.i. Display Resolution

The number of voxels of the proposed 3D fog display can be formulated as follows. Recall that M_0 is the horizontal pixel dimension on the front plane that we measured during Step 3 of calibration in Section II.B. We first need to express M_0 in terms of d. Without loss of generality, we assume the xy aspect ratio of the volumetric display $W : H$ is not smaller than the aspect ratio of the projector $M : N$. We assume the projection area covers the entire display volume, that is, $M \geq M_0$. Thus,

$$M_0 = \frac{MW}{2d\tan\frac{\theta_x}{2}} \tag{6}$$

The display resolution (or total number of voxels) V of our system is formulated as the total pixel resolution of all n image planes. An intuitive understanding of the relation between d and V is that shorten the projection distance can increase the number of pixels being displayed on each image planes, thus enhancing the display resolution. To formally demonstrate this, we express the display resolution V as a function of projection distance d based on (4) and (6):

$$V(d) = \sum_{j=1}^{n} M_j^2 N_j^2 = \sum_{j=1}^{n} s_j^2 M_0^2 \frac{H}{W} = \sum_{j=1}^{n} \frac{M^2 WH}{4(d+l_j)^2 \tan^2\frac{\theta_x}{2}} \tag{7}$$

Thus, $V(d)$ is strictly decreasing.

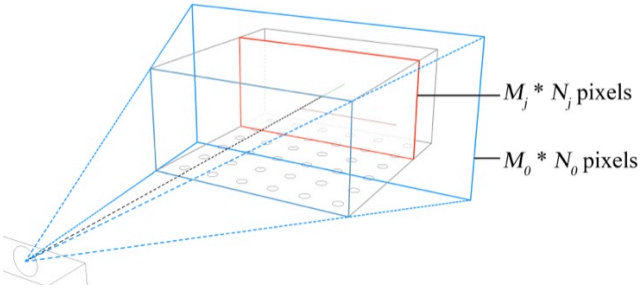

Figure 5. Image resolution of image plane j is reduced from $M_0 * N_0$ to $M_j * N_j$

D.ii. Critical Projection Distance

When the projector is placed very close to the fog screen, there is a possibility that more than one fog elements cast the same image point. As illustrated in Fig. 6(a), we define a distance called the critical projection distance $d_{critical}$ given by

$$d_{critical} = \frac{1}{2}[\delta_z(m-2)(n-1)-L] \tag{8}$$

When $d = d_{critical}$, $f_{m-1} = 1$ and $f_m = n$ (or similarly $f_1 = n$ and $f_2 = 1$), the projection line passes through two activated fog elements at the same time. This makes the two image segments overlap and the projected light to be scattered by both fog columns. To avoid fog occlusion and this undesirable artifact, the projector should be moved away from the fog screen beyond $d_{critical}$ (Fig. 6(b)). We will give an illustrative example in Section III.C. to demonstrate the occlusion phenomenon.

D.iii. Optimal Solution

The optimal projection distance d^* can be obtained by maximizing the display resolution $V(d)$ under constraints:

$$d^* = \arg\max_d V(d) \tag{9}$$

$$\text{subject to} \quad d > d_{critical} \tag{10}$$

$$d \geq \frac{W}{2\tan\frac{\theta_x}{2}} \tag{11}$$

$$d \geq \frac{H}{2\tan\frac{\theta_y}{2}} \tag{12}$$

Constraints (11) and (12) are based on the requirement that the entire display volume needs to be covered by the projection volume. According to (7), $V(d)$ is strictly decreasing. Thus, the optimal projection distance d^* equals to the largest value among the three lower bounds for d:

$$d^* = \max\left\{\frac{1}{2}[\delta_z(m-2)(n-1)-L],\ \frac{W}{2\tan\frac{\theta_x}{2}},\ \frac{H}{2\tan\frac{\theta_y}{2}}\right\} \tag{12}$$

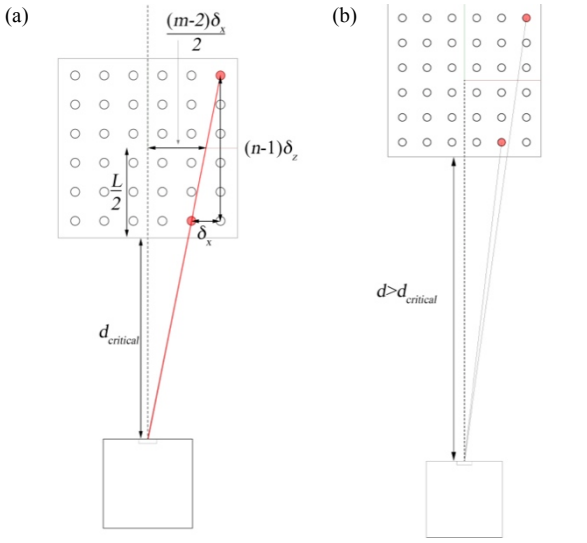

Figure 6. Image occlusion occurs when $d \leq d_{critical}$.

D.iv. Projector's Depth of Field

The projector's focus is set to produce the sharpest image on the world xy-plane, where its depth of field is comparable to or larger than the depth of the display volume D such that the projected image is acceptably sharp within the entire volume. Moving the projector further away from the fog screen can increase the depth of field. However, it will significantly reduce the display resolution based on (7). The depth of field of the projector will also constrain the depth of the display volume. In our case, the image remains clear on both front and rear planes even when $d < d^*$. Thus, we do not impose an additional constraint for d to achieve a larger depth of field.

III. Experiments

We have implemented the methods presented above and developed a software in Processing [16] to conduct the experiments. Our projector model is ASUS P2B that has an official throw ratio 1.1 (i.e. $\theta_x = 48.8°$, $\theta_y = 31.7°$) and native resolution 1280 by 800 pixels. The measured fov is $\theta_x = 46.9°$, $\theta_y = 30.4°$. The fog display has a high tolerance to off-axis view. The off-axis viewangle is around ±20°. Thus, the overall horizontal observable angle of the display is around ±45° from the principal axis. Our prototype display contains *6* by *6* closely packed fog emitters, where the nozzle distance is $\delta_x = \delta_z = 65.25mm$. The dimensions of display volume are *W:402.5mm* by *L:402.5mm* by *H:200mm*, *H* is the measured fog height. Based on these metrics, we obtained the system's critical projection distance $d_{critical} = 451.25mm$. However, the optimal projection distance should be *463mm* due to (11). In the first two examples, the projector was placed at around $d = 550mm$. Each fog emitter is controlled by an Arduino Mega board using the serial data sent from Processing. Three sets of experiments are presented below.

A. Displaying Static Objects

In the first experiment, we extensively used the Stanford bunny model as visuals to test our display with different fog configurations. First, we tested its performance using single and multiple fog emitters to display one image object. As shown in Fig. 7(a), a small sized bunny model was projected on the fog produced from a single fog emitter. The bunny image appeared to be very clear with high quality of 3D details. We then projected three bunny models onto the fog produced by three different emitters as shown in Fig. 7(b). The bunnies were precisely projected at distinct physical locations. As our display allows a wide off-axis viewangle, their actual positions in the space can be naturally perceived by many users at the same time.

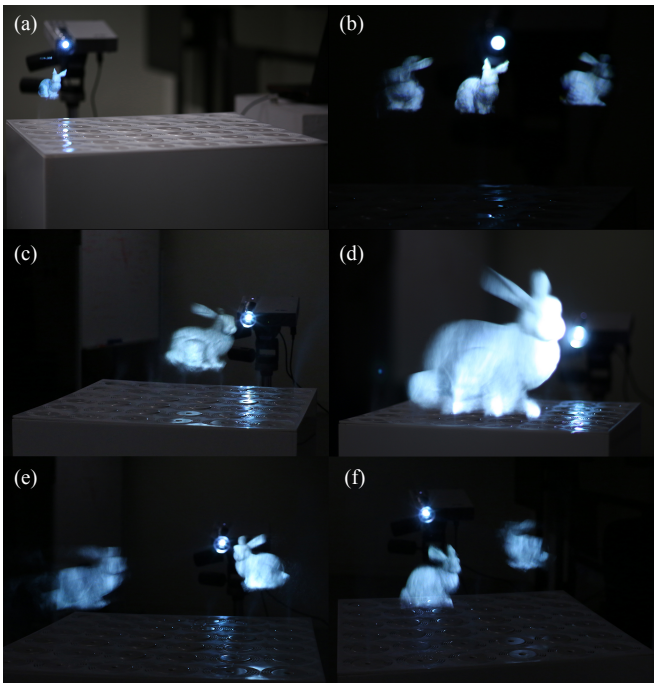

Figure 7. Static objects of various size shown with different fog screen configurations: (a) small sized model using one fog emitter (b) three small sized models at different locations (c) one medium sized model using three fog emitters (d) one big model using six fog emitters (e)&(f) two medium sized models at different locations.

The fog emitters can also be combined to create a larger fog screen to display large objects. In Fig. 7(c-f), three and six emitters in same row were used simutaneously to display larger bunny models. This demonstated the capability of the system in displaying objects of a wide range of scale. Moreover, all tests verified that our image transformation

method can precisely scale and translate the objects to their desired sizes and positions in the display volume.

B. Displaying Dynamic Objects

The performance of displaying dynamic content was tested by using an animated gif of the famous bistable optical illusion called the Spinning Dancer [17]. Rather than just spinning around at a fixed location, the figure was given a planned roundtrip, 3D path to travel within the display volume. The trajectory was represented by translation in image coordinate together with a fog vector *f* to define the *z* position in every frame. The system used *f* to switch the fog emitter matrix. When the dancer traveled between different depth levels, the software resized the image so that there would not be size distortion. Fig. 8 and the video attachment demonstrated the good 3D display quality and nice continuity of moving.

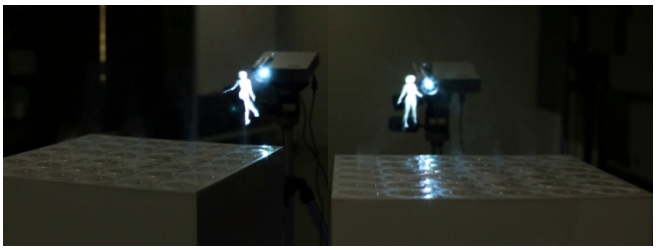

Figure 8. Animated figure travelling in a 3D path in the fog display.

C. Verification of Critical Projection Distance

To illustrate the concept of fog occlusion and critical projection distance as described in Section III.D.ii. and Fig. 6, we performed a test to display the same 3D content with two different projection distances. We created a scenrio: a red square was to be projected at the fog in the 1st column and the 6th row, and a white circle to be projected at the fog in the 2nd column and the 1st row. Thus, the fog emitters at these two position were switched on. We first placed the projector close to the display so that $d < d_{critical}$. Fig. 9(a) shows that both patterns appeared at both positions because the projection rays overlaped and the fog screen failed to separate the patterns. When we incresed d so that $d > d_{critical}$, the two patterns did not overlap and could be formed at two distinct locations as shown in Fig. 9(b). This proved that the critical projection distance can avoid the overlapping artifacts.

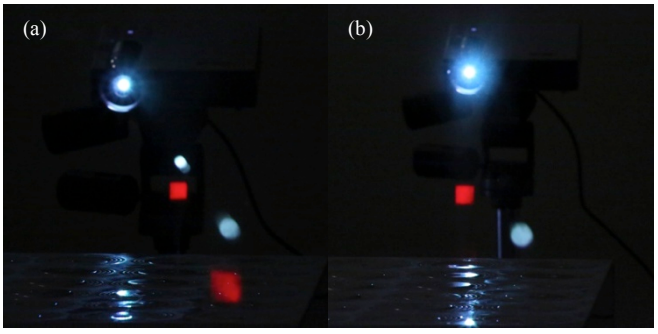

Figure 9. Comparison of the different projection distance.

IV. Future Works and Concluding Remarks

This paper has presented a novel volumetric display that projects a 2D image onto a non-planar, reconfigurable fog screen. The proposed display creates image in mid-air in the real physical space thus creating immersive, true 3D experience. The current design of the proposed 3D fog display has low resolution in *z*-direction. It can be improved by replacing the non-moving fog emitter arrays with a set of linear stages while each moving one fog emitter in *z*-direction precisely [18]. We will test using multiple projections from two or four directions to further enhance the range of viewangles. The most powerful feature of 3D immaterial display is the potential to create new interesting possibilities for tangible interaction and the interplay between virtual and physical objects. We will use a number of motion or gesture sensing devices, such as infrared camera, Leap Motion and Kinect, with the fog display system to facilitate touch, reach-through interaction and augmented reality.

References

[1] A. Jones, I. McDowall, H. Yamada, M. Bolas, and P. Debevec, "Rendering for an interactive 360 light field display," *ACM Transactions on Graphics (TOG),* vol. 26, p. 40, 2007.

[2] K. Ito, H. Kikuchi, H. Sakurai, I. Kobayashi, H. Yasunaga, H. Mori*, et al.*, "Sony raymodeler: 360º autostereoscopic display," in *ACM SIGGRAPH Emerging Technologies*, 2010.

[3] E. Gregg, "Volumetric 3d displays and application infrastructure," *IEEE Computer Society,* vol. 8, pp. 37-44, 2005.

[4] H. Kimura, T. Uchiyama, and H. Yoshikawa, "Laser produced 3d display in the air," in *ACM SIGGRAPH Emerging technologies*, 2006, p. 20.

[5] H. Saito, H. Kimura, S. Shimada, T. Naemura, J. Kayahara, S. Jarusirisawad*, et al.*, "Laser-plasma scanning 3d display for putting digital contents in free space," in *Electronic Imaging 2008*, 2008, p. 680309.

[6] Y. Ochiai, T. Hoshi, and J. Rekimoto, "Three-dimensional mid-air acoustic manipulation by ultrasonic phased arrays," *PloS one,* vol. 9, p. e97590, 2014.

[7] Y. Ochiai, T. Hoshi, and J. Rekimoto, "Pixie dust: Graphics generated by levitated and animated objects in computational acoustic-potential field," *ACM Transactions on Graphics (TOG),* vol. 33, p. 85, 2014.

[8] S. Follmer, D. Leithinger, A. Olwal, A. Hogge, and H. Ishii, "Inform: Dynamic physical affordances and constraints through shape and object actuation," in *Uist*, 2013, pp. 417-426.

[9] S. DiVerdia, I. Rakkolainena, T. Höllerera, and A. Olwala, "A novel walk-through 3d display," in *SPIE Stereoscopic Displays and Virtual Reality Systems*, San Jose, California, USA, 2006.

[10] S. Suyama, S. Ohtsuka, H. Takada, K. Uehira, and S. Sakai, "Apparent 3-d image perceived from luminance-modulated two 2-d images displayed at different depths," *Vision Research,* vol. 44, pp. 785-793, 2004.

[11] C. Lee, S. DiVerdi, and T. Hollerer, "Depth-fused 3d imagery on an immaterial display," *Visualization and Computer Graphics, IEEE Transactions on,* vol. 15, pp. 20-33, 2009.

[12] A. Yagi, M. Imura, Y. Kuroda, and O. Oshiro, "360-degree fog projection interactive display," in *SIGGRAPH Asia Emerging Technologies*, 2011, p. 19.

[13] P. C. Barnum, S. G. Narasimhan, and T. Kanade, "A multi-layered display with water drops," *ACM Transactions on Graphics (TOG),* vol. 29, p. 76, 2010.

[14] Arduino. Available: http://www.arduino.cc/

[15] D. Moreno and G. Taubin, "Simple, accurate, and robust projector-camera calibration," in *3DIMPVT*, 2012, pp. 464-471.

[16] Processing. Available: http://processing.org/

[17] Spinning dancer. Available: http://en.wikipedia.org/wiki/Spinning_Dancer

[18] M.-L. Lam, B. Chen, K.-Y. Lam, and Y. Huang, "3d fog display using parallel linear motion platforms," in *International Conference on Virtual Systems and Multimedia (VSMM2014)*, 2014.